Journal of Leather Science and Engineering

RESEARCH Open Access

Amphiphilic hyperbranched polymers: synthesis, characterization and self-assembly performance

Longfang Ren[1,2*], Qiaoxuan Niu[1,2], Jing Zhao[1,2] and Taotao Qiang[1,2]

Abstract

A series of amphiphilic hyperbranched polymers (AHP-s, the "s" refers to the algebra of AHP) were synthesized by the reaction between hydroxyl-terminated hyperbranched polymers (HBP-s, the "s" refers to the algebra of HBP) and palmitoyl chloride. FTIR, NMR and GPC were used to determine the structure of AHP-s, the results showed that AHP-s exhibits core-shell structure. The thermal properties of polymers were investigated by DSC and TGA. It was found that AHP-2, AHP-3 and AHP-4 display higher thermal stability than AHP-1 (AHP-1, AHP-2, AHP-3 and AHP-4 represent the first, second, third and fourth generation AHP, respectively). Furthermore, the self-assembly performance of AHP-s in THF solvent was investigated by TEM and SEM. Finally, the encapsulation capacity of the AHP-s for methyl orange (MO) was explored at different concentrations of AHP-s and pH conditions. It was found that AHP-s is capable of accommodating hydrophilic guest MO. Moreover, the higher generation of AHP-s, the stronger encapsulation capacity obtained. And the encapsulation capacity closely associated with the pH of encapsulation system.

Keywords: Amphiphilic Hyperbranched polymers, Synthesis, Self-assembly, Guest encapsulation performance

1 Introduction

The incompatibility of the hydrophilic and lipophilic segments on amphiphilic polymer causes microphase separation to occur making the amphiphilic polymer exhibit self-assembly characteristics in selective solvent, bulk and surface, interface structures [1, 2]. Hyperbranched polymers have attracted great attentions due to their specific spheroid-like shape and multi-functionality, which can be modified to obtain new supramolecular structural materials [3–5]. Up to now, various amphiphilic hyperbranched polymers have been prepared through hydrophilic or lipophilic modified hyperbranched polymers [6–9], such as hyperbranched multiarm star polymers, linear–hyperbranched polymers and hyperbranched-graft polymers [10, 11]. Amphiphilic hyperbranched polymers have both hyperbranched structural properties and performance advantages of amphiphilic polymers. However, the synthesis of amphiphilic hyperbranched polymers whose structure can be controlled is very scarce. Uncontrollable structures lead to poor repeatability of the results. The commonly used ring-opening polymerization and atom transfer radical polymerization (ATRP) synthesis processes are uncontrollable and cannot effectively control the self-assembly behavior of molecules. Cheng et al. [12] proposed a kind of uncontrollable hyperbranched polymer with the amphiphilic core synthesized by ring-opening polymerization of glycerol, using palmitoyl chloride to graft core to obtain the amphiphilic hyperbranched polyglycerols. Nevertheless, the process of ring-opening polymerization is uncontrollable, resulting that the prepared amphiphilic polymers exhibit uncontrolled self-assembly characteristic.

Self-assembly is an area of considerable interest due to the potential value in catalysis, reaction vessels, drug delivery and so forth [13]. Hyperbranched polymers are drawing more and more attention especially in the fields of self-assembly owing to their specific size, shape and properties. Many impressive supermolecucular aggregates at all scales and dimensions have been obtained

* Correspondence: renlf1010@163.com
[1]College of Bioresources and Materials Engineering, Shaanxi University of Science & Technology, Xi'an 710021, Shaanxi, China
[2]National Demonstration Center for Experimental Light Chemistry Engineering Education, Shaanxi University of Science & Technology, Xi'an 710021, China

[14–16], such as unimolecular micelles, polymer vesicles, composite vesicles and macroscopic tubes. Further research about amphiphilic hyperbranched polymers have been demonstrated unique advantages in supramolecular self-assembly behaviors, including special properties, unique self-assembly mechanisms and functionalization processes. As well-known, the amphiphilic hyperbranched polymers which can be control the structure possess great significance in certain particular field. Yan et al. [17] reported self-assembly behavior of amphiphilic hyperbranched polymers with hydrophilic hyperbranched core and hydrophobic linear arms. However, the inverted unimolecular micelle in organic solvent is uncontrollable, which is unfavourable for its further application research.

Herein, we present the synthesis and self-assembly performance of amphiphilic hyperbranched polymers with a controllable hydrophilic core and hydrophobic alkyl shell of high grafting ratio. It can be controlled molecular structure by adjusting the proportion of reactants to change molecular algebra and the ratio of the amphiphilic. Such amphiphilic hyperbranched polymers with a controllable hydrophilic core are expected to display a specific self-assembly behavior depending on solvents. Furthermore, the encapsulation property of amphiphilic hyperbranched polymers to MO was also investigated. It was found that synthetic amphiphilic hyperbranched polymer can capture the water-soluble small molecule MO dye insoluble in chloroform into the pores of the polymer, which is expected to be used as a dispersion and transport medium for aqueous dyes in oily media.

2 Experimental section

2.1 Materials

The succinic anhydride ($C_4H_4O_3$) and palmitoyl chloride ($C_{16}H_{31}ClO$) were provided by Aladdin reagent. Methanol (CH_3OH), trimethylolpropane ($C_6H_{14}O_3$), sodium chloride (NaCl) and Sodium hydroxide (NaOH) were purchased from Tianjin Hengxing Chemical Co., Ltd. Diethanolamine ($C_4H_{11}NO_2$) and pyridine (C_5H_5N) was supplied by Tianjin Tianli Chemical Reagent Co., Ltd.p-toluenesulfonic acid (p-$CH_3C_6H_4SO_3H$) was obtained from Tianjin Guangfu Fine Chemicals. Chloroform ($CHCl_3$) was purchased from Shanghai Macklin Biochemical Technology Co., Ltd. Methylene chloride (CH_2Cl_2), methyl orange (MO) and tetrahydrofuran (THF) were provided by Tianjin kemiou Chemical Reagent Co., Ltd. All reagents used were analytical grade. And all experimental drugs can be used directly.

2.2 Synthesis of amphiphilic hyperbranched polymers (AHP-s)

The amphiphilic hyperbranched polymers (AHP-s) were synthesized by the reaction between hydroxyl-terminated hyperbranched polymers (HBP-s) and palmitoyl chloride. In a typical synthesis, succinic anhydride (0.01 mol, 1.00 g) and methanol (10 mL) were mixed at a three-necked flask. Then, diethanolamine (0.01 mol, 1.05 g) was added dropwise with vigorous stirring and the reaction was continued for 6 h at ice-water bath condition. After the reaction, the methanol was removed under reduced pressure to obtain AB_2 monomer. After that, trimethylolpropane (0.005 mol, 0.67 g) and pyridine (10 mL) were mixed in four-necked flask under nitrogen atmosphere, then p-toluenesulfonic acid (2%, based the total mass of the reaction system) was added with vigorous stirring, the AB2 monomer was added dropwise to the reaction bottle, the mixture was allowed to react for 8 h at 120 °C. Different generations of HBP-s were synthesized with molar ratios of trimethylolpropane to AB2 monomer 1:3, 1:9, 1:21, 1:43, which was denoted as HBP-1, HBP-2, HBP-3, and HBP-4, respectively. Specific synthetic process was shown in Fig. 1.

AHP-s is synthesized with palmitoyl chloride and HBP-s. For instance, the specific synthesis process of AHP-2 as follows: HBP-2 (1.24 g, containing about 0.01 mol reactive hydroxy), pyridine (10 mL) and chloroform (10 mL) were placed in the reaction flask with vigorous stirring under nitrogen atmosphere. After the mixture was dissolved, palmitoyl chloride (0.012 mol, 3.30 g) was added rapidly with vigorous stirring, the mixture solution was stirred for 10 h at 60 °C. After that, the solvent was removed on a rotary evaporator to obtain the crude products. Then, the crude products were dissolved in methylene chloride and were washed with deionized water three times to remove pyridine hydrochloride. Finally, the organic phase was collected and the solvent was removed on a rotary evaporator, and the final product was dried under vacuum at 40 °C for 2 days to obtain pale yellow solid powder (AHP-2, 2.16 g). Specific synthetic process was shown in Fig. 2.

The different generations of amphiphilic hyperbranched polymers were obtained by the same method, the products were marked as AHP-1, AHP-2, AHP-3 and AHP-4, rspectively. The AHP-1 shows a pale yellow sticky solid, whereas, AHP-2, AHP-3 and AHP-4 display a pale yellow solid powder.

2.3 Characterization

The HBP-2, AHP-2 powder and KBr powder were dried in a vacuum oven at 70 °C for 6 h, and the KBr tableting technique was employed, the FTIR spectrum was recorded on a VECTOR-22 FTIR spectrometer (BRUKER Co, Germany) at the scanning range of 4000~500 cm^{-1}, the number of scans is 32 times. ^1H and ^{13}C NMR spectra were performed at 25 °C on a Varian INOVA 500 MHz spectrometer (BRUKER Co, Germany), the AHP-s was dried in a vacuum oven at 70 °C for 6 h, approximately 15 mg of the sample was placed in a nuclear

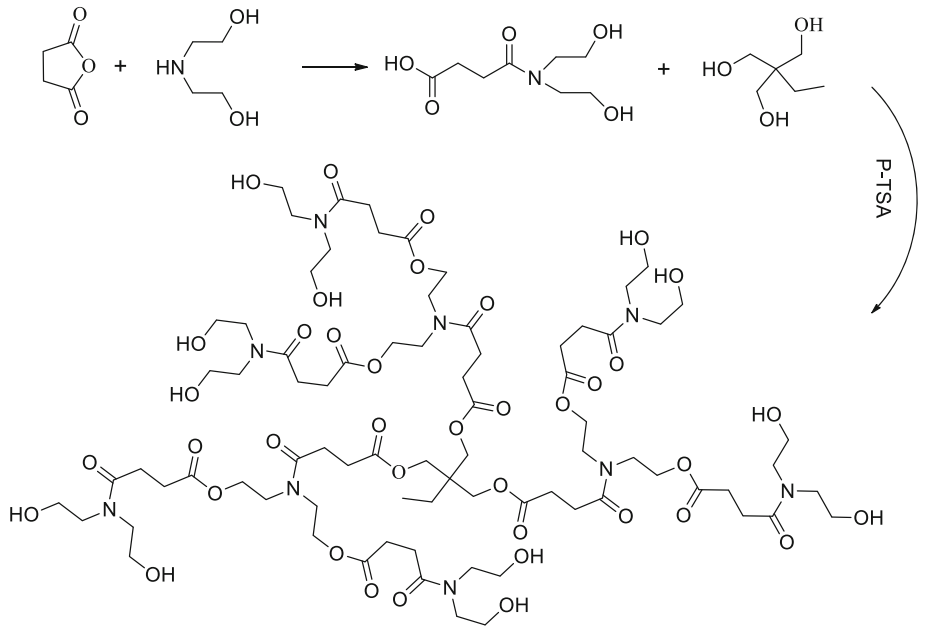

Fig. 1 Synthesis process of HBP

magnetic tube and dissolved with 0.6 mL of CDCl3, and the number of scans was 32. Gel Permeation Chromatography (GPC) of the AHP-s was detected using a Waters 515–2414 system (Waters Co, American) at the flow rate of 1.0 mL min^{-1}. The conventional column was calibrated with polystyrene (PS), furthermore, freshly distilled THF was employed as an eluent at 25 °C. Differential scanning calorimetry (DSC) measurements were analyzed by a DSC-204 (NETZSCH Co, Germany), the temperature range was 20 to 120 °C at a heating rate of 10 °C·min^{-1} and nitrogen flow rates of 40 mL·min^{-1}. Thermogravimetric analysis (TGA) was collected on a TGA Q500 (TA Co, American) in the temperature range of 30–600 °C at a heating rate of 10 °C·min^{-1} and nitrogen flow rates of 40 mL·min^{-1}. Transmission electron microscopy (TEM) measurement was performed on a JEM-2100 instrument operating at voltage of 100 kV. Scanning electron microscope (SEM) was carried out on

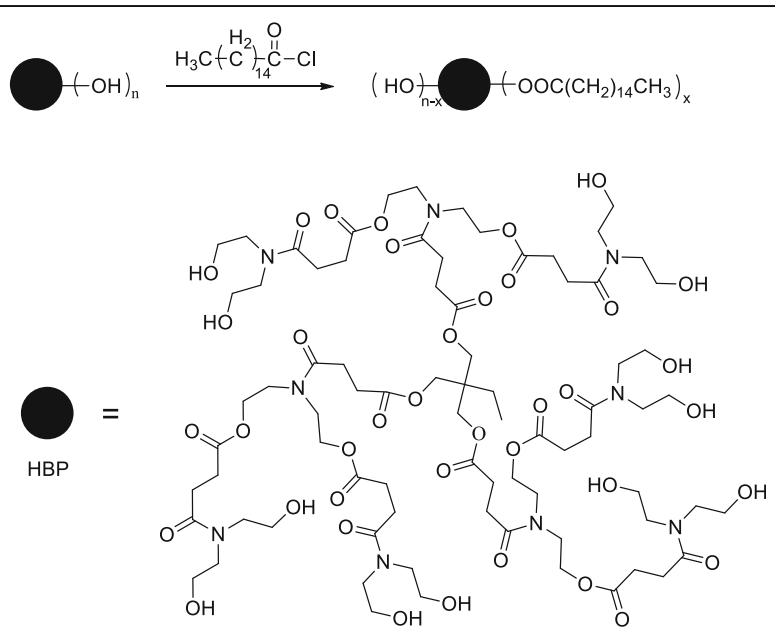

Fig. 2 Synthesis process of AHP-s

a S4800 instrument operating at a voltage of 5 kV. Dynamic light scattering tests (DLS) was performed on a nanoparticle size surface potential analyzer (Malvern Co, Britain). UV-vis spectra were obtained from UV-265 FW UV-vis Spectrophotometer (Shimadzu Co, Japan).

2.4 Self-assembly experimental method in THF

5 mg AHP-2 was dissolved in 5 mL THF at room temperature with the concentration of 1.0 mg·mL^{-1}. A drop of AHP-2 solution was dropped onto copper grid covered graphite, after the solvent evaporation, the microstructure observation was performed on a JEM-2100 Transmission electron microscopy instrument operating at a voltage of 100 kV. In addition, a drop of AHP-2 solution was dropped onto silicon wafer, after the solvent evaporation, the observation of microstructure was carried out on a S4800 scanning electron microscope instrument operating at a voltage of 5 kV. Place the configured solution in a cuvette and perform particle size analysis using a nanoparticle size surface potential analyzer.

2.5 Methodology for dye extraction phase transfer processes

The chloroform solution of the AHP-s (0.01 to 0.5 g·L^{-1}) was mixed with the same volume of MO dye aqueous solution. The mixed solution was shaken for 10 min and equilibrated at room temperature in a dark chamber for 24 h. The dye concentration was adjusted to make sure that only a part of the dye was transferred from aqueous solution into $CHCl_3$ phase. The chloroform phase was measured by UV-vis spectrophotometry to determine the absorbance of solution. Taking AHP-2 as an example, the morphological changes of AHP-2 chloroform solution (0.5 g•L-1) before and after encapsulation to MO were observed by SEM and TEM, the changes of AHP-s aggregate size before and after encapsulation were further detected by DLS.

2.6 Phase transfer experiment under different pH

The pH value of MO in deionized water is 6.6. HCl and NaOH aqueous were used to regulate the pH value of MO aqueous solution to expected value. Then the MO aqueous solution with certain pH value was mixed with AHP-2 chloroform solution and shook for 10 min. Allow to stand layering to obtain aqueous phase and $CHCl_3$ phase. And HCl and NaOH aqueous were used to adjust the pH of the water phase into expected value. The solution was shaken for 10 min and kept in dark chamber at room temperature for 24 h prior to measure. The concentrations of dye in water were invariable, whereas the AHP-2 chloroform solution was adjusted until only a part of the dye in water was transferred into the CHCl3 phase.

3 Results and discussion

3.1 Characterization of amphiphilic hyperbranched polymers

The structure of the obtained AHP-s was confirmed by FTIR, ^{1}H NMR, and ^{13}C NMR. Herein, we choose AHP-2 as an example to characterize the chemical properties of AHP-s, and the detailed analysis as follows.

Figure 3 shows the FTIR spectra of AHP-2, it can be seen that the characteristic peaks of obtained AHP-2 are different from the unmodified HBP-2. Compare to HBP-2, the stretching vibration peak of -OH with broad absorption band at 3382.53 cm^{-1} becomes weakened in AHP-2. And the absorption peak of -CH_2- at 2950.55 cm^{-1} is significantly strengthened. That is because the -OH group of HBP-2 is replaced by long-chain alkyl. In addition, the signals at 1792.83 cm^{-1} and 1625.70 cm^{-1} which belong to the stretching vibration of -COO- and -CON- appeared in both HBP-2 and AHP-2, but the absorption peak of -CON- in AHP-2 was significantly weaker than the absorption peak of HPB-2. Because the reaction of grafting increases the molecular weight of AHP-2, and results in a decrease of the -CON- content in AHP-2.However, the grafting reaction also forms new -COO-, so the absorption peak of the -COO- is no significant changes with molecular weight's increasation. The above results indicate that the amphiphilic hyperbranched polymer was synthesized successfully by the modification reaction.

The ^{1}H NMR and ^{13}C NMR spectra further indicate the microstructure of AHP-2. The ^{1}H NMR spectra of AHP-2 was shown in Fig. 4, and it can be confirmed that AHP-2 was successfully synthesized. Symbol "1~4" represents the characteristic peaks of proton in the hydrophilic core of AHP-2. The proton peak "1" around δ = 4.01~4.21attribut to methylene protons connected with

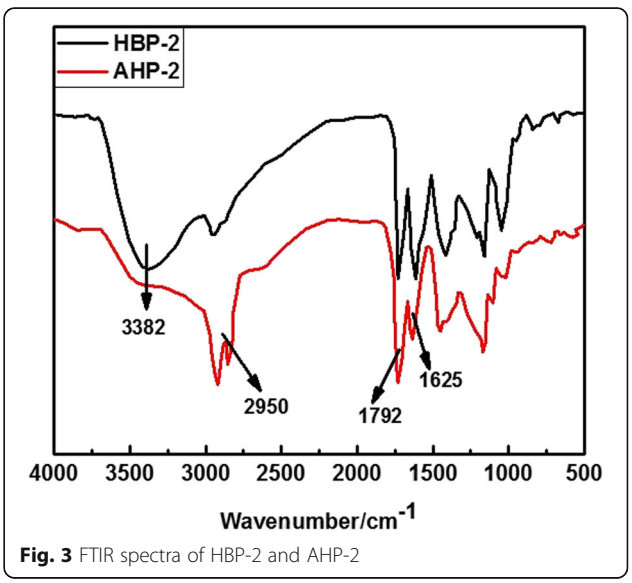

Fig. 3 FTIR spectra of HBP-2 and AHP-2

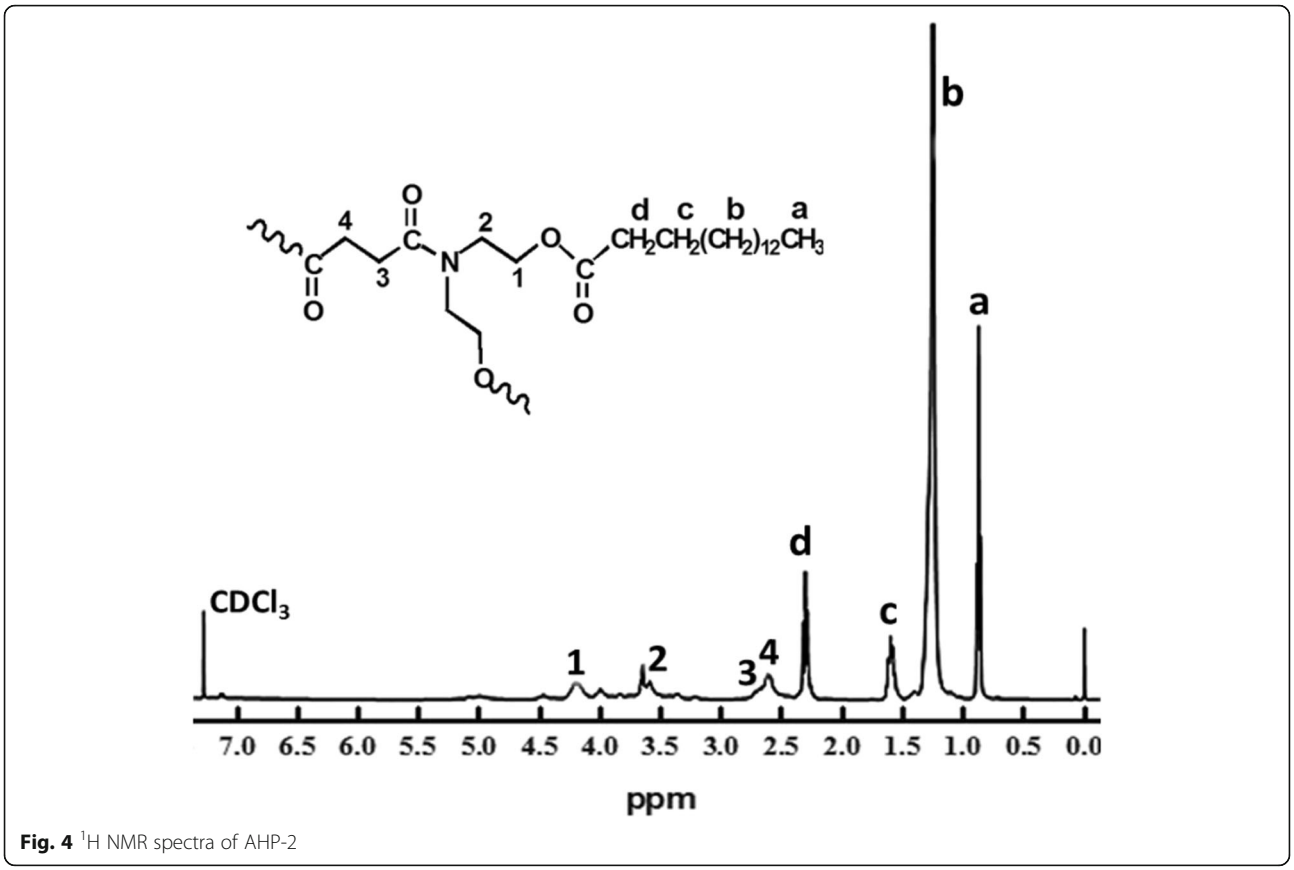

Fig. 4 ^{1}H NMR spectra of AHP-2

oxygen of ester-based, The proton peak "2" around δ = 3.67 belong to methylene protons connected with nitrogen of amide, The proton peak "3" around δ = 2.63 belongs to methylene protons connected with carbon of amide, the proton peak "4" around δ = 2.70 attach to methylene protons connected with carbon of ester-based. Symbols "a~d" denote signals of alkyl chains. Proton peak "a" around δ = 0.86~0.89 is assigned to methyl protons of hexadecyl, and the proton peak "b" around δ = 1.26 is attributed to methylene protons of hexadecyl. Moreover, there are a large number of methylene-linked resulting the overall performance of the absorption peak is the wide peak, the proton peak "c" around δ = 1.57~1.64 corresponds to secondary methylene protons connected with carbon of ester-based in hexadecyl chains, the proton peak "d" around δ = 2.30~2.34 is assigned to methylene protons of hexadecyl connected with carbon of ester-based. The grafting ratio (J) of the different generation polymers can be calculated by hydroxyl value of the polymers, the expression is shown in Eq. (1):

$$J = (A_0 - A_1)/A_0 \quad (1)$$

Wherein, A_0 and A_1 refer to the hydroxyl value of HBP and AHP, respectively.

The determination of hydroxyl value is according to the previous literature [18], and the calculated J values of different generation polymers are shown in Table 1.

Figure 5 gives the ^{13}C NMR spectra of AHP-2. The signal "1" around δ = 14.14 is assigned to methyl carbon of hexadecyl in HAP-2, and the absorption peak "2" around δ = 22.72 indicates methylene carbon which connected with methyl of alkyl chains. The absorption peak "3" around δ = 24.83 is correspond to secondary

Table 1 Characteristics of different generation AHP-s

Polymer	Grafting Ratio (%)	DB	Theoretical M_n (g·mol^{-1})	M_n(g·mol^{-1})	M_w(g·mol^{-1})	M_w/M_n	T_g (°C)
AHP-1	97.4	0.51	1304.41	1591.59	1924.62	1.21	27.2
AHP-2	96.2	0.55	3036.28	2645.01	3624.67	1.37	29.3
AHP-3	95.6	0.61	9798.46	5208.92	7919.57	1.52	30.7
AHP-4	93.1	0.63	20,024.38	9568.15	15,789.10	1.65	32.1

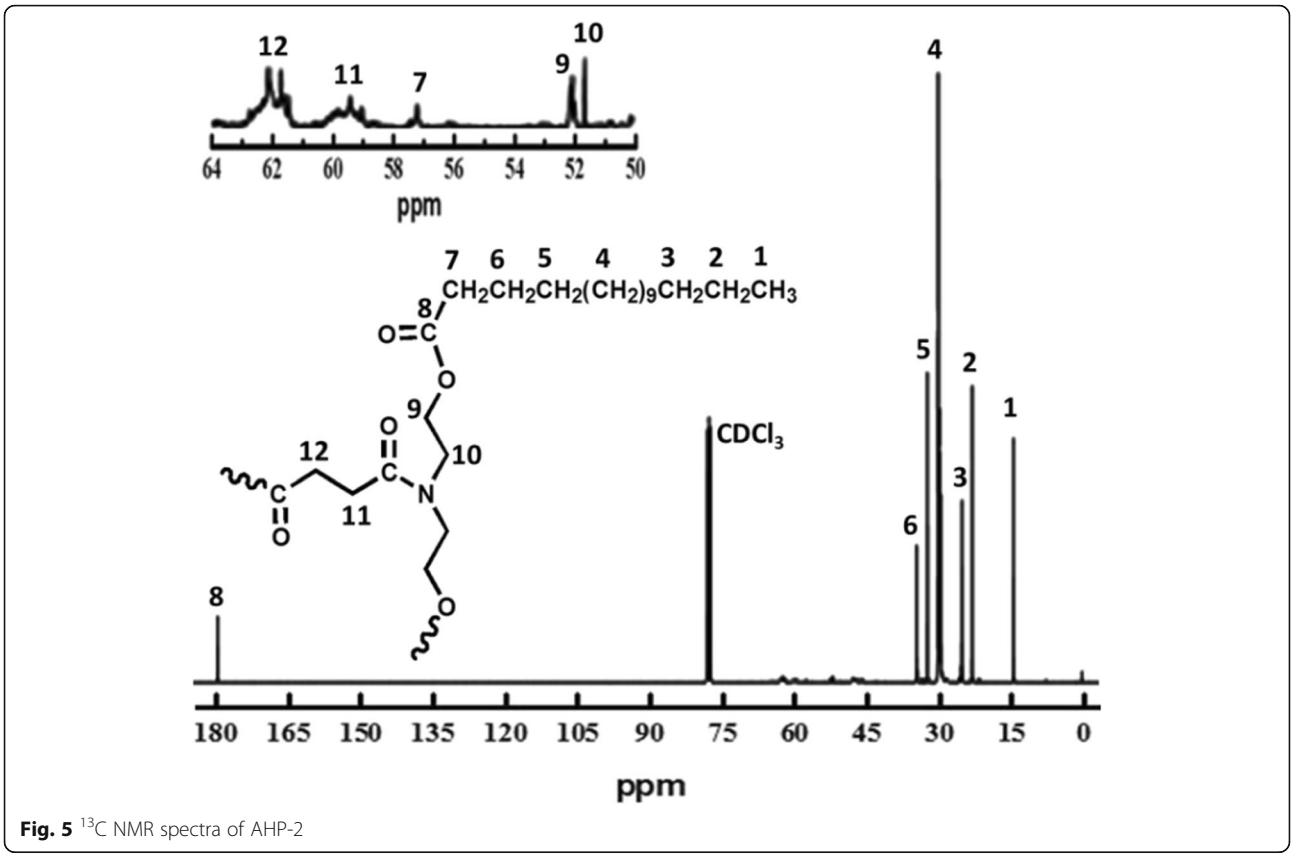

Fig. 5 ^{13}C NMR spectra of AHP-2

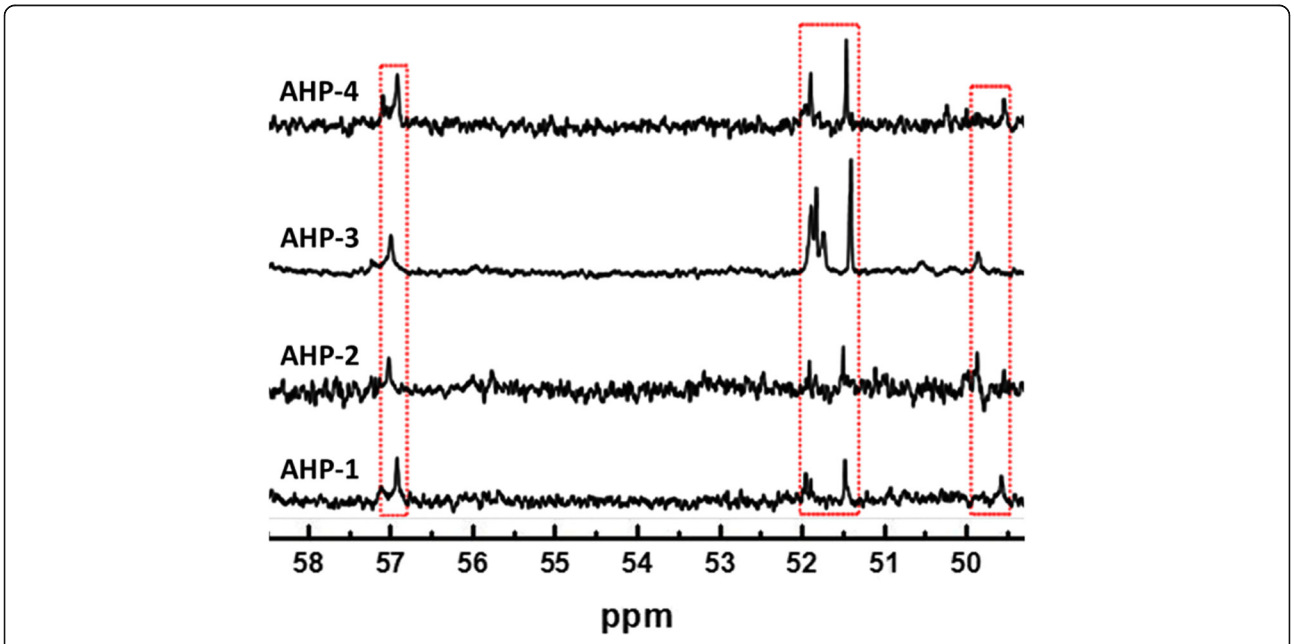

Fig. 6 ^{13}C NMR spectra of the different generation AHP-s

methylene carbon which connected with methyl of alkyl chains in AHP-2. The signal "8" around δ = 178.78 represents the ester group carbon of hexadecyl in AHP-2. The signal "7" δ = 57.05 indicates methylene carbon which connected with ester-based carbon in hexadecyl. "6" δ = 57.05 is correspond to secondary methylene carbon which connected with ester-based carbon in hexadecyl. And "5" δ = 31.96 belongs to the third methylene carbon which connected with ester-based carbon in hexadecyl. The signal "4" around 29.17~29.74 belongs to the other methylene carbon of hexadecyl. The absorption peak at δ = 50.00–65.00 ppm corresponds to the absorption peak of carbon in the hydrophilic core. The absorption peak of carbon in the hydrophilic core is not obvious which is attributed that the $CDCl_3$ is selected as the deuterated solvent. The test results indicate that the product structure contains palm alkyl chain and the target product is obtained.

Figure 6 is the ^{13}C NMR spectra of the different generation polymers. The absorption peak δ = 49.72, δ = 51.39~51.81 and δ = 56.91 are correspond to the dendritic unit (D), linear unit (L) and terminal unit (T) of the polymers, respectively. The degree of branching (DB) is determined according to the previous literature [19], and the calculated formula of DB is shown in Eq. (2):

$$DB = (D + T)/(D + T + L) \quad (2)$$

The results are displayed in Table 1. It is clear that the DB of the polymers is gradually increased with the growth of generations. The DB of one generation products is just 0.51, which means that the structure of polymers is not perfect spherical structure. However, the DB of other products is higher than one generation products, which means the structure of polymers is more perfect spherical structure.

The molecular weight of AHP-s is detected by GPC, and the results are shown in Table 1. As can be seen from the results, the experimentally measured molecular weights were lower than the theoretical values obtained from the idealized models, which indicate that synthesized AHP-s has less perfect chemical microstructure, and the molecular weight distribution is gradually increasing and irregular with the increase of generations. The synthesis of hyperbranched polymers is different from traditional linear condensation polymer, the highly branched structure leads to the relative molecular weight and molecular weight distribution of hyperbranched polymers are not in conformity with the classic polycondensation reaction rule. On the other hand, because PS standard-based GPC measurements underestimate the molecular weight of hyperbranched polymers, a discussion of those differences on a quantitative level is meaningful.

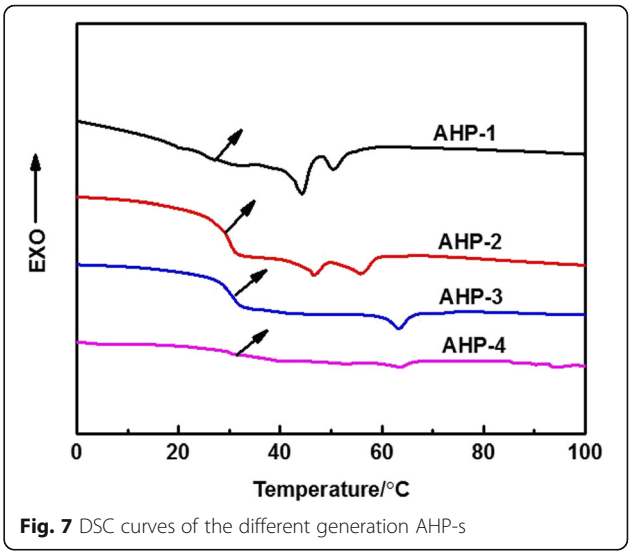

Fig. 7 DSC curves of the different generation AHP-s

3.2 Thermal properties of amphiphilic hyperbranched polymers

In general, the glass transition of hyperbranched polymers is different from the traditional linear polymers. Hyperbranched polymers exhibit a large number of terminal functional groups which will affect the glass transition temperature (T_g) of hyperbranched polymers. However, it does not reflect the flexibility and free volume of the movement unit, but reflects the interaction of the terminal functional groups [20, 21].

The DSC of the AHP-s is shown in Fig. 7. The results of T_g of AHP-s are displayed in Table 1. As can be seen from the results, the T_g of AHP-s is gradually increased with the increase of relative molecular weight. As for

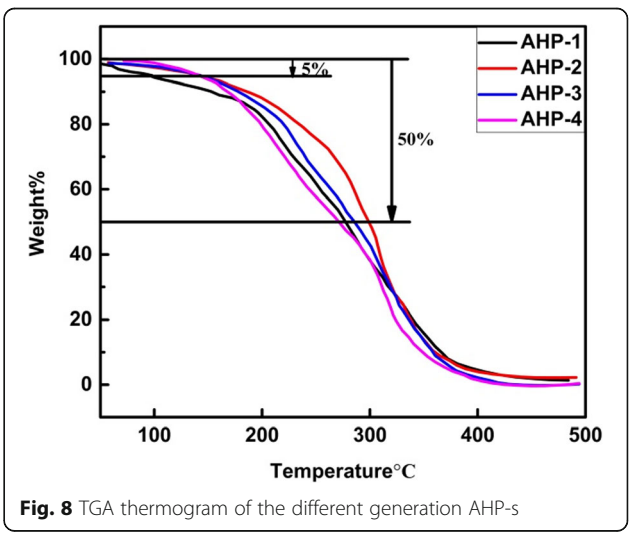

Fig. 8 TGA thermogram of the different generation AHP-s

higher generation AHP-s, the number of the terminal groups is much larger than the lower generation AHP-s, so that the interaction between terminal groups gradually increases. As a result, the T_g of AHP-s was gradually increased. Secondly, there are obvious 1~2 melting peaks in AHP-s. There are many possible reasons, such as different crystal forms or different levels of perfection wafers [22]. The core and shell structures of AHP-s both are shown the melting of the respective crystals in this paper. At the same time, as the algebra increases, the melting peak moves toward high temperature and gradually disappears. This is because the proportion of AHP-s polar hydrophilic nuclei increases with the algebra increases, the interaction between molecules increases, the molecules need absorbed more energy at a higher temperature to break away from the intermolecular forces and achieve the characteristics of free movement. The gradual disappearance of the melting peak further indicates that the polymer is amorphous, and the higher the degree of branching of the polymer, the lower crystallization.

The TGA thermogram of the AHP-s is shown in Fig. 8. It can see that the temperature is about 100 °C when thermal weight loss 5% for AHP-1, and other AHP-s is about 150 °C. The decomposition rate of AHP-1 is significantly than AHP-2, AHP-3 and AHP-4 before 150 °C. The weight loss of AHP-1 is the most and with lower thermal stability. The reason is that the molecular weight of AHP-1 is small, and the peripheral alkyl chain is not tightly packed, So the -COO-、-CON- of molecule were decomposed earlier.

AHP-2, AHP-3 and AHP-4 have more higher thermal decomposition rate between 300~400 °C.The reason is that the ratio of peripheral alkyl groups in the molecule is decreased with the algebra increase, so the thermal stability decreases. The change between AHP-s after 400 °C is not obvious, that because AHP-s mostly have decomposed before 400 °C.

3.3 Self-assembly of amphiphilic hyperbranched polymers in THF

The different structure of the AHP-s can lead to different self-assembled aggregates in selective solvents [8, 23]. The obtained AHP-s has a distinct core-shell structure. The hydroxyl-core act a strong hydrophilic property compared to alkyl-shell, which cause a specific self-assembled behavior in given solvent and generate a particular morphologies of micelle aggregation.

The TEM image was used to represent the morphology of AHP-s in THF solvent (as shown in Fig. 9). As can be seen from the TEM image, the different generation AHP-s can form the micellar aggregation of various sizes and morphologies in THF. Moreover, the lower generation AHP-s generates single molecular

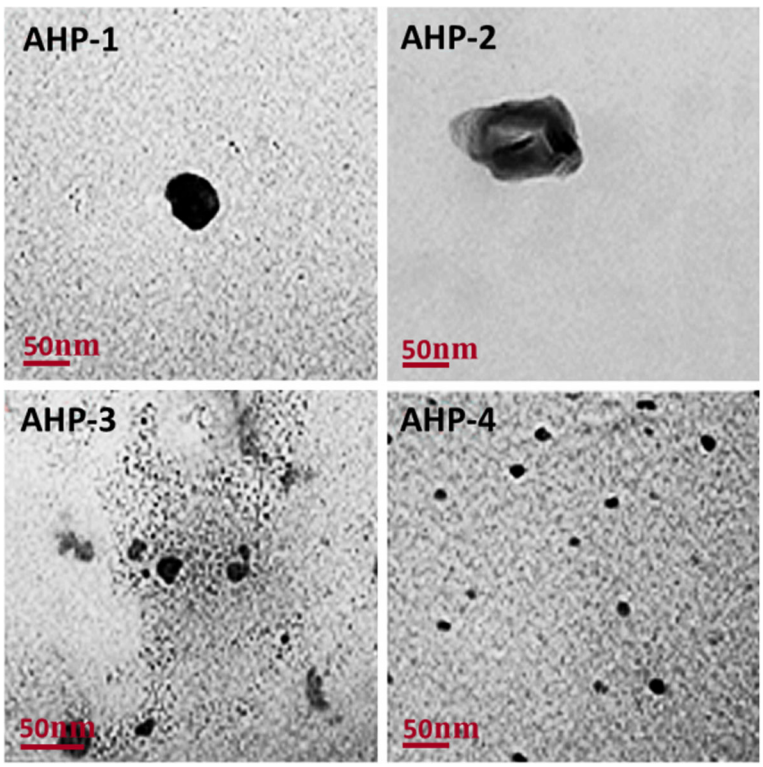

Fig. 9 TEM image of the different generation AHP-s in THF

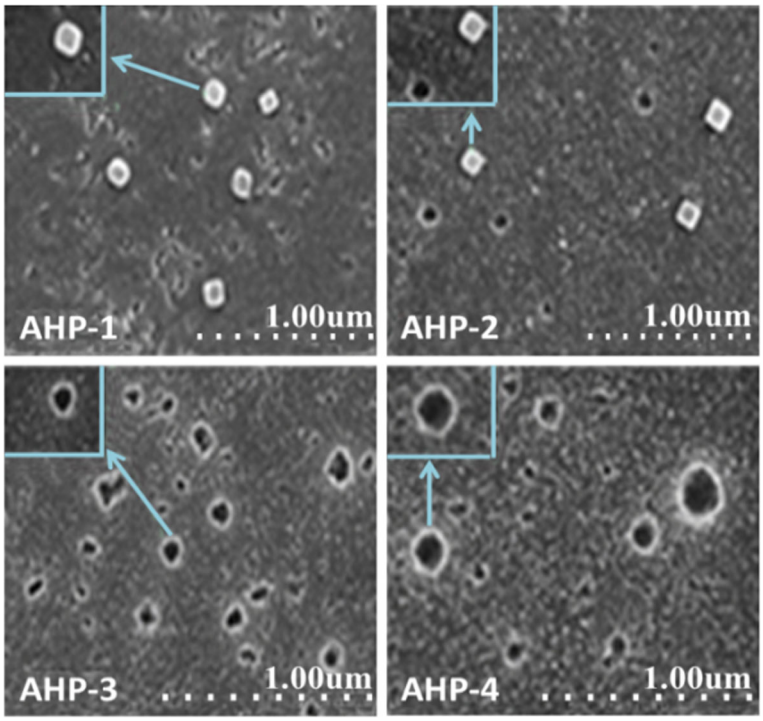

Fig. 10 SEM image of the different generation AHP-s in THF

micelle, and the diameter of those aggregations is about 20 nm. Meanwhile, the higher generation AHP-s can not only obtain the single molecular spherical micelle but also the multimolecular micelles can be formed, and the diameter of those aggregations is at the range of 20 nm to 50 nm. In addition, Figure of AHP-2 depicts the core-shell structure of the micelle obviously. In concrete, the internal of micelle (about 50 nm) is the spherical hydrophilic core, and the external of micelle (about 20 nm) is the hydrophobic alkyl-chain shell.

The SEM image of the different generation AHP-s in THF is shown in Fig. 10. It can be seen from the figure, the first generation AHP-s can form the spherical single molecule micelle, and the diameter of that aggregation is about 20 nm. Nevertheless, the higher generation AHP-s can form spherical single molecular micelle, multi-molecular micelle and polymer vesicles, and the diameter of those aggregations is from 20 to 80 nm.

DLS (Fig. 11) shows the size of AHP-s aggregates formed in THF. It can be seen that as the algebra increases, the particle size of AHP-s increases gradually from 51 nm to 164 nm, which because the self-assembly performance of different generations AHP-s have affected by the structure of polymers. The structure of lower generation AHP-s is not perfect, and the external shell closely surrounds the internal hydrophilic core, which results in AHP-s forming the single molecule micelle in THF. However, the higher generation AHP-s possess a large number of hydrophobic alkyl-chains whose interaction are more tightness, so that it can form a multi-molecular aggregation and polymer vesicles in THF solvent.

3.4 Phase transfer mechanism

The obtained AHP-s showed interior hydrophilic hydroxyl-core and exterior hydrophobic alkyl-shell in apolar solvent which are expected to display an inverted micellar behavior [24]. The shell structure derived from

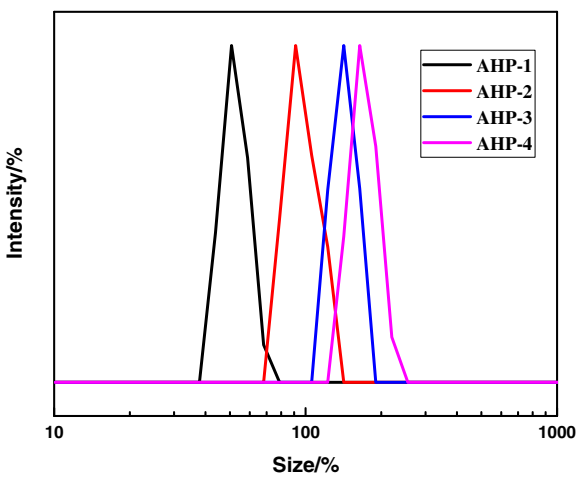

Fig. 11 DLS image of the different generation AHP-s in THF

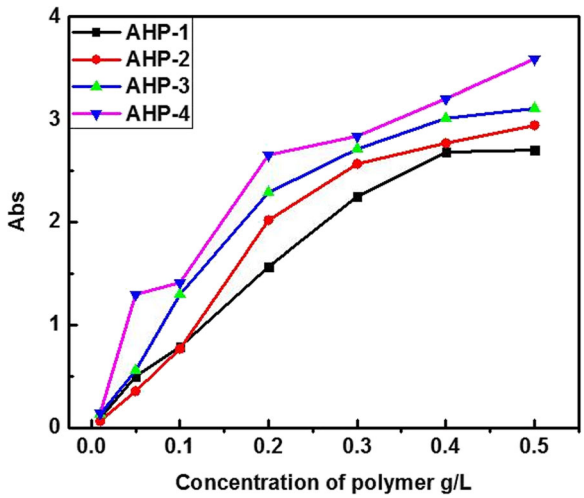

Fig. 12 The MO encapsulation capacity of AHP-s with different concentration

hydrophobic alkyl chain, which is benefit for the stabilization of the interface between hydrophilic hydroxyl-core and external apolar solvent. Therefore, the guest encapsulation behaviors of the obtained AHP-s were investigated in this paper. Firstly, the typical water-soluble anionic dye methyl orange (MO) was used as a probe to demonstrate the micellar property of the AHP-s. The normal liquid-liquid extraction protocol was adopted: an aqueous solution of MO dye was mixed with the same volume of chloroform solution of AHP-s. The dyes were encapsulated by polymer, meanwhile, the organic phase turns colored, which leads to the increase of dyes concentration in chloroform solvent.

The encapsulation capacity of AHP-s to MO in different concentration is shown in Fig. 12. As depicted in Fig. 12, the encapsulation capacity of AHP-s to MO is gradually increased with the increase of AHP-s concentration. Moreover, it is obvious that the increase of the encapsulation capacity is faster at the beginning, and the guest loading achieved equilibrium when the AHP-s concentration reached 0.4 g/L. On the other hand, the encapsulation capacity of different generation AHP-s to MO is also different, the encapsulation capacity of the lower generation AHP-s is worse than higher generation AHP-s. The phenomena discussed above can be explained as following. Firstly, with the increase of the AHP-s concentration, the AHP-s can aggregate as micellar and the number of the accommodating guest molecules is increased. Secondly, the guest molecules can strongly interact with the hydroxyl-core through hydrogen-bonding and electrostatic interactions. In addition, with the increase of the size and polarity of the hydroxyl-core, the higher generation AHP-s can supply more space to accommodate the guest molecules [25]. Besides, the higher generation AHP-s possess more hydroxyl groups, which leads to the interaction between dyes and polymers is more closely than the lower generation AHP-s.

The SEM and TEM images of AHP-2 before and after encapsulation are shown in Figs. 13 and 14. SEM shows that AHP-2 has a spherical micelle morphology before encapsulation, however, the micelles size increases and some micelles tend to be ellipsoid after AHP-2 encapsulating MO, which because the hydrophilic dye enters the inside of the micelle, causing the AHP-2 to be assembled again. In the process, the micelles change from a relatively stable sphere to an ellipsoid. Compared the TEM and DLS (as shown in Fig. 15) before and after encapsulation, the size of micelles particles increased from about 30 nm to 60 nm. This is because the hydrophilic MO dye enters the micelle to the balance of the micelles is broken. The particles need more molecules to provide more space to maintain a stable encapsulation of

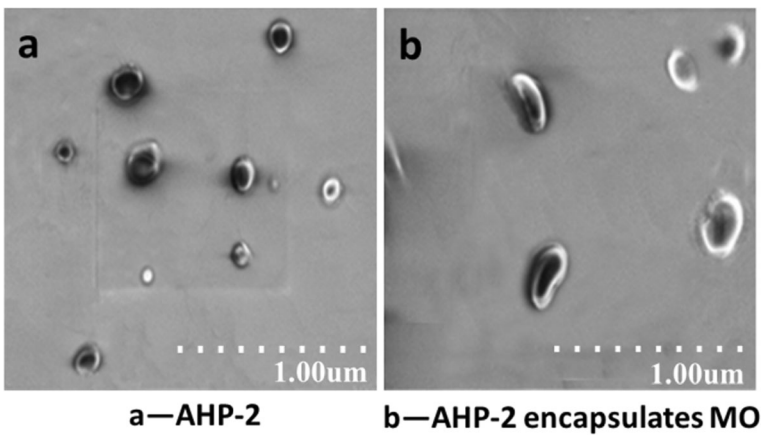

Fig. 13 SEM image before and after AHP-2 encapsulates MO dye

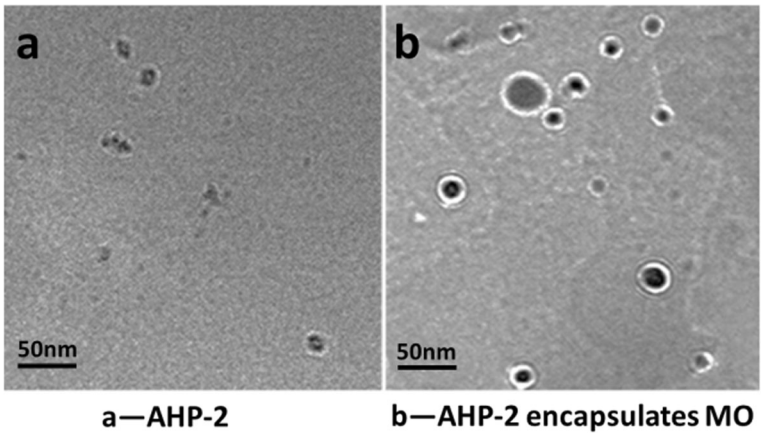

Fig. 14 TEM image before and after AHP-2 encapsulates MO dye

the internal hydrophilic MO dye. The hydrophilic hydroxyl-core can supply a microenvironment for the accommodation of hydrophilic guest molecules due to their similar polarities, hence, AHP-s can be used as a carrier to make the hydrophilic guest molecules can be dissolved in nonpolar solvent [26]. The unique encapsulation behavior of AHP-s in THF for MO is expected to be a good dispersant for aqueous dyes in oily media.

3.5 Phase transfer mechanism under different pH

The encapsulation capacity of AHP-s to MO under different pH is shown in Fig. 16. According to the Fig. 16, the guest loading rate is decreased with the pH increased from 2.6 to 10.6, which is contributed by the protonation of hydroxyl under acidic condition. Therefore, the dyes can interact with the polymers closely under acidic condition due to electrostatic interaction. The higher-generation AHP-s with larger hydrophilic cores has the better encapsulation ability. At the same time, it can be seen that the pH have less effect on the encapsulation capacity of higher-generation AHP-s, because the higher-generation AHP-s have more hydrophobic alkyl groups at the periphery, forming a tighter shell layer, resulting in the core to be better surrounded. Therefore, the higher-generation AHP-s still exhibit high encapsulation capabilities at high pH conditions.

4 Conclusions

A series of hyperbranched polymers (AHP-s) with amphiphilic core-shell structure were successfully synthesized. TGA analysis indicated that the thermal stability of high-generation AHP-s was higher than the AHP-1. In addition, SEM and TEM showed that different generations of AHP-s can self-assembled to form different micelle morphology in THF. The higher generation AHP-s can form single molecular micelle,

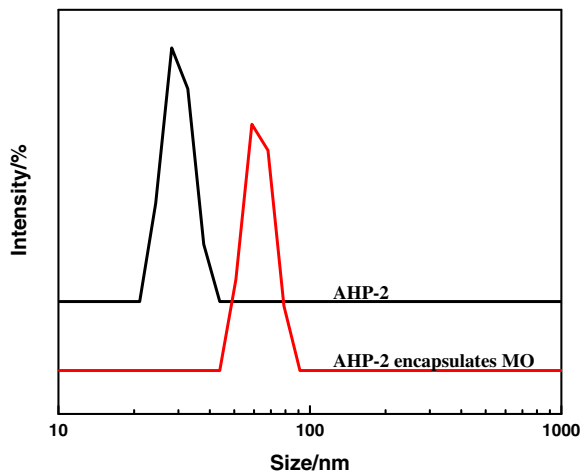

Fig. 15 DLS image before and after AHP-2 encapsulates MO dye

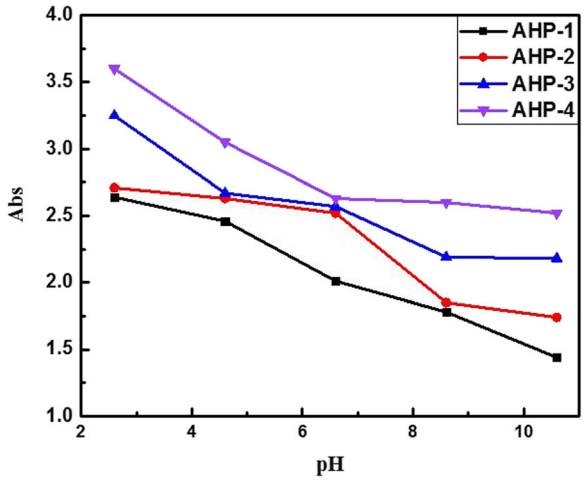

Fig. 16 The MO encapsulation capacity of AHP-s under different pH condition

multimolecular micelle and polymer vesicles due to the existence of abundant alkyl chain. Finally, the encapsulation capacity of the AHP-s to MO showed that AHB-s is meaningful for studying the loading and release of hydrophilic guests in non-polar solvents. And the guest encapsulation capacity can be affected by the size of the amphiphilic hydroxyl core and pH conditions, the higher algebra of AHP-s, the lower pH is, the higher loading rate can be obtained.

Acknowledgements
This work was funded by National Science and Technology Major Project (No. 2017YFB0308500), Shaanxi Science and Technology Project (No. 2018JM5164), Science and Technology Plan Project of Xi'an Weiyang District (No. 201907) and the Youth Innovation Team of Shaanxi Universities.

Authors' contributions
RLF and QTT conceived and designed the study. NQX and ZJ performed the experiments and analyzed the experiments data. RLF, QTT, NQX and ZJ reviewed and edited the manuscript. All authors read and approved the manuscript.

Funding
This work was funded by National Science and Technology Major Project (No. 2017YFB0308500), Shaanxi Science and Technology Project (No. 2018JM5164), Science and Technology Plan Project of Xi'an Weiyang District (No. 201907) and the Youth Innovation Team of Shaanxi Universities.

Availability of data and materials
All data and material generated or analyzed during this study are included in this published article. The authors declare that the data in this article is reliable.

Competing interests
The authors declare that they have no competing interests.

Received: 12 April 2019 Accepted: 12 November 2019
Published online: 06 February 2020

References

1. Wu G, Chen SC, Liu CL, et al. Direct aqueous self-assembly of an amphiphilic diblock copolymer toward multistimuli-responsive fluorescent anisotropic micelles. ACS Nano. 2015;9:4649–59. https://doi.org/10.1021/acsnano.5b01370.
2. Wu G, Chen SC, Zhan Q, et al. Well-defined amphiphilic poly (p-dioxanone)-grafted poly (vinyl alcohol) copolymers: Synthesis and micellization. J Polym Sci. 2010;48:4811–22. https://doi.org/10.1002/pola.24272.
3. Gao C, Yan DY. Hyperbranched polymers: from synthesis to applications. Prog Polym Sci. 2004;29:183–275. https://doi.org/10.1016/j.progpolymsci.2003.12.002.
4. Huang H, et al. Facile modification of nanodiamonds with hyperbranched polymers based on supramolecular chemistry and their potential for drug delivery. J Colloid Interf Sci. 2017;513:198–204. https://doi.org/10.1016/j.jcis.2017.11.009.
5. Konkolewicz D, Monteiro MJ, Perrier J. Dendritic and hyperbranched polymers from macromolecular units: elegant approaches to the synthesis of functional polymers. Macromolecules. 2011;44:7067–87. https://doi.org/10.1021/ma200656h.
6. Tan H, et al. Dissipative particle dynamics simulation study on phase diagrams for the self-assembly of amphiphilic hyperbranched multiarm copolymers in various solvent conditions. Soft Matter. 2017;13. https://doi.org/10.1039/C7SM01170A.
7. An SG, Li GH, Cho CG. Synthesis of amphiphilic star block copolymers of polystyrene with PEG core via ATRP—control of chain architecture and the formation of core–shell type globular structure. Polymer. 2006;47:4154–62. https://doi.org/10.1016/j.polymer.2006.02.041.
8. Wurm F, Schüle H, Frey H. Amphiphilic linear-hyperbranched block copolymers with linear poly (ethylene oxide) and hyperbranched poly (carbosilane) block. Macromolecules. 2008;41:9602–11. https://doi.org/10.1021/ma8018427.
9. Skey J, et al. Synthesis and self-assembly of amphiphilic chiral poly(amino acid) star polymers. Macromolecules. 2010;43:5949–55. https://doi.org/10.1021/ma101019g.
10. Zhang X, Wang H, Yu D. Biodegradable amphiphilic graft polymer synthesized via the combination of ring-opening polymerization (ROP) and atom transfer radical polymerization (ATRP). Mater Lett. 2017;198:144–7. https://doi.org/10.1016/j.matlet.2017.03.154.
11. Wu G, Chen SC, Wang XL, et al. Dynamic origin and thermally induced evolution of new self-assembled aggregates from an amphiphilic comb-like graft copolymer: a multiscale and multimorphological procedure. Chem A Eur J. 2012;18:12,237–41. https://doi.org/10.1002/chem.201103961.
12. Cheng H, et al. Synthesis and self-assembly of amphiphilic hyperbranched polyglycerols modified with palmitoyl chloride. J Colloid Interf Sci. 2009;337:278–84. https://doi.org/10.1016/j.jcis.2009.05.026.
13. Wu G, Chen SC, Zhan Q, et al. Well-defined amphiphilic biodegradable comb-like graft copolymers: their unique architecture-determined LCST and UCST thermoresponsivity. Macromolecules. 2011;44:999–1008. https://doi.org/10.1021/ma102588k.
14. Zhang ZH, et al. Synthesis of unimolecular micelles with incorporated hyperbranched boltorn H30 polyester modified with hyperbranched helical poly(phenyl isocyanide) chains and their enantioselective crystallization performance. Macromol Rapid Commun. 2017;38:1700315. https://doi.org/10.1002/marc.201700315.
15. Samuel AZ, Ramakrishnan S. *Janus* Hybramers: Self-adapting amphiphilic hyperbranched polymers. Macromolecules. 2012;45:2348–58. https://doi.org/10.1021/ma2022277.
16. Schömer M, Seiwert J, Frey H. Hyperbranched poly(propylene oxide): A multifunctional backbone-thermoresponsive olyether polyol copolymer. ACS Macro Lett. 2012;**1**:888–91. https://doi.org/10.1021/mz300256y.
17. Yan D, Zhou Y, Hou J. Supramolecular self-assembly of macroscopic tubes. Science. 2004;303:65–7. https://doi.org/10.1126/science.1090763.
18. Kojima C, et al. Synthesis and characterization of hyperbranched poly (glycidol) modified with pH- and temperature-sensitive groups. Bioconjugate Chem. 2009;20:1054–7. https://doi.org/10.1021/bc900016x.
19. Fossum E. Book review of hyperbranched polymers: synthesis, properties, and applications. J Am Chem Socie. 2011;133:14,840. https://doi.org/10.1021/ja207716g.
20. Min XU, Tan K, Zhou HJ, et al. Effect of terminal groups on the properties of hyperbranched polymers. J Functional Polymers. 2003;**16**:299–303. https://doi.org/10.1007/BF02974893.
21. Farias ED, Passeggi MCG, Brunetti V. Thermal transitions in hyperbranched polyester-polyol assemblies on carbon. Eur Polym J. 2018;102:68–74. https://doi.org/10.1016/j.eurpolymj.2018.03.021.
22. Ye HM, Chen XT, Liu P, et al. Prominently promoting the formation of poly(butylene adipate) α -form crystals by coalescing from inclusion complex. Chin J Polymer Sci. 2018;36:1–5. https://doi.org/10.1007/s10118-018-2095-x.
23. Cheng H, et al. Effect of degree of branching on the self-assembly of amphiphilic hyperbranched multiarm copolymers. Macromolecules. 2010;43:1143–7. https://doi.org/10.1021/ma902452p.
24. Wan D, et al. Can Nonspecific host-guest interaction lead to highly specific encapsulation by a supramolecular nanocapsule? Macromolecules. 2009;42:6448–56. https://doi.org/10.1021/ma900952e.
25. Liu Y, et al. A supramolecular hyperbranched polymer with multi-responsiveness constructed by pillar[5]arene-based host–guest recognition and its application in the breath figure method. Mater Chem Front. 2018;2:1568–73. https://doi.org/10.1039/C8QM00220G.
26. Pu WF, et al. Water-soluble core–shell hyperbranched polymers for enhanced oil recovery. Ind Eng Chem Res. 2015;54:798–807. https://doi.org/10.1021/ie5039693.

Publisher's Note